



Coordinated Control of Doubly Fed Induction Generator Virtual Inertia and Power System Oscillation Damping Using Fuzzy Logic

A. R. Solat^a, A. M. Ranjbar^b, B. Mozafari^{*a}

^a Department of Electrical and Computer Engineering, Science and Research Branch, Islamic Azad University, Tehran, Iran

^b Department of Electrical Engineering, Sharif University of Technology, Tehran, Iran

PAPER INFO

Paper history:

Received 31 December 2018

Received in revised form 02 February 2019

Accepted 07 March 2019

Keywords:

Doubly Fed Induction Generator Wind Turbine

Virtual Inertia Control

Frequency Stability

Inter-area Oscillation

Fuzzy Logic

ABSTRACT

Doubly-fed induction generator (DFIG) based wind turbines with traditional maximum power point tracking (MPPT) control provide no inertia response under system frequency events. Recently, the DFIG wind turbines have been equipped with virtual inertia controller (VIC) for supporting power system frequency stability. However, the conventional VICs with fixed gain have negative effects on inter-area oscillations of regional networks. To cope with this drawback, this paper proposes a novel adaptive VIC to improve both the inter-area oscillations and frequency stability. In the proposed scheme, the gain of VIC is dynamically adjusted using fuzzy logic. The effectiveness and control performance of the adaptive fuzzy VIC is evaluated under different frequency events such as loss of generation, short circuit disturbance with load shedding. The simulation studies are performed on a generic two-area network integrated with a DFIG wind farm and the comparative results are presented between three cases: DFIG without VIC, DFIG with fixed gain VIC, and DFIG with adaptive fuzzy VIC. All the results confirm the proposed fuzzy VIC can improve both the inter-area oscillations and frequency stability.

doi: 10.5829/ije.2019.32.04a.11

NOMENCLATURE

Wind Turbine		Synchronous Generator	
H_t, H_g	Turbine and generator inertia constants	P_m, P_e	Mechanical and electrical powers
ω_t, ω_r	Turbine and generator angular speed	ω, δ	rotor angular speed and position
$c_{sh}, k_{sh}, \theta_{tw}$	Damping, stiffness and twist angle of shaft	ω_0	rated angular speed of power system
ω_{eb}, ω_s	Electrical base and synchronous speed	H, D	Inertia and damping coefficients
T_m, T_e	Mechanical and electrical torques	Abbreviations	
i_{sd}, i_{sq}	d and q axis stator currents	DFIG	Doubly-fed induction generator
v_{rd}, v_{rq}	d and q axis rotor voltages	VIC	Virtual inertia controller
E'_d, E'_q	d and q axis voltages behind transient reactance	MPPT	Maximum power point tracking
R_s, R_r	Stator and rotor resistances	GSC	Grid side converter
L_s, L_r, L_m	Stator, rotor and mutual inductances	RSC	Rotor side converter
L'_s	Stator transient inductance	GA	Genetic algorithm
$T_r = L_r / R_r$	Rotor time constant	ITAE	integral time-weighted absolute error

* Corresponding Author Email: mozafari@srbiau.ac.ir (B. Mozafari)

1. INTRODUCTION

During the last years, an increase in environmental pollution and decrease in fossil fuel reserves have attracted more attention to generate the electric power using renewable and clean energies. Among the various resources, wind energy has fastest growth due to the widespread availability and economic and technical reasons. Initially, wind power was generated using squirrel cage induction generator (SCIG). Today, however, DFIG is the most commonly used technology in wind power systems. It is a wound rotor induction generator that are joined to the network with stator directly and rotor through power electronic converters. The DFIG provides variable speed performance for extracting maximum wind power and flexible control of reactive and active powers [1, 2].

However, the DFIG with traditional MPPT control provides no inertial response during the system frequency events such as load shedding, loss of generation, and etc. [3]. The inertial response directly affects the initial rate of frequency deviation so that the power systems with lower inertia are more prone to the frequency instability [4]. Therefore, with increasing the penetration of DFIG-based wind farms, there are major concerns about the power system frequency stability [5, 6]. Recently, the potential of variable speed wind turbine for improving the system frequency stability has been addressed by a variety of VICs [7]. The most common method is to employ a supplementary signal proportional to df/dt which is added to the reference of DFIG's active power control loop [8, 9]. This derivative controller can emulate an inertial response for DFIG using the stored kinetic energy in the turbine rotor [10]. In this scheme, a first-order high-pass filter is also used to activate the VIC only when there are impressive frequency deviations [11, 12]. Note that because of the wider speed regulation range, the DFIGs equipped with the VIC may provide better frequency support compared to the conventional synchronous generators [4].

On the other hand, some of studies [13-15] have concluded that the reduced inertia of power systems due to the increased penetration of DFIG wind farms improves the power systems oscillations damping. Beyond this, Miao et al. [16] have revealed that the virtual inertia control of DFIG worsens the damping of power system oscillations. The study conducted by Xi et al. [17] also confirms that providing more virtual inertia by DFIG reduces the power system oscillations damping. To overcome this difficulty, the present study proposes an adaptive VIC for DFIG wind turbines which is not only provides promising inertia response during frequency events but also can improve the inter-area oscillations of regional networks. To achieve this purpose, a fuzzy logic based control system is designed

for dynamically adjusting the virtual inertia gain with respect to the system oscillations.

The remainder of the paper is sectioned as: In section 2, a brief description of DFIG wind turbine and VIC model is presented. In section 3, the relationship between the system inertia and oscillation damping is analysed and subsequently the proposed VIC is designed using fuzzy logic. In section 4, performance of the proposed fuzzy VIC is verified using simulation studies. Finally, the main findings of the study are presented in section 5.

2. DFIG WIND TURBINE WITH VIC

2. 1. The Model of DFIG Wind Turbine The general structure of a DFIG wind turbine together with its controllers is shown in Figure 1(a). It consists of turbine, drive-train, generator, power electronic converters and control blocks. The turbine gets the kinetic energy of wind and delivers it in the form of rotating mechanical torque. Subsequently, the extracted mechanical torque is transmitted to the generator through a drive-train system. Also, the generator is a wound rotor induction generator that both the stator and rotor are jointed to the grid. In power system stability studies, very fast electric transients of the stator are usually disregarded and the system is modeled in the form of a voltage source behind a transient impedance [18]. The model of mechanical and electrical systems is given as follows,

Mechanical system:

$$2H_t \frac{d\omega_t}{dt} = T_m - k_{sh} \theta_{tw} - c_{sh} \frac{d\theta_{tw}}{dt} \quad (1)$$

$$\frac{1}{\omega_{eb}} \frac{d\theta_{tw}}{dt} = \omega_t - \omega_r \quad (2)$$

$$2H_g \frac{d\omega_r}{dt} = k_{sh} \theta_{tw} + c_{sh} \frac{d\theta_{tw}}{dt} - T_e \quad (3)$$

Electrical system:

$$\frac{dE'_d}{dt} = \omega_{eb} \left[\omega_s \frac{(L_s - L'_s)}{T_r} i_{sq} + \omega_s (\omega_s - \omega_r) E'_q - \frac{E'_d}{T_r} - \frac{\omega_s L_m}{L_r} v_{rq} \right] \quad (4)$$

$$\frac{dE'_q}{dt} = \omega_{eb} \left[-\omega_s \frac{(L_s - L'_s)}{T_r} i_{sd} - \frac{E'_q}{T_r} - \omega_s (\omega_s - \omega_r) E'_d - \frac{\omega_s L_m}{L_r} v_{rd} \right] \quad (5)$$

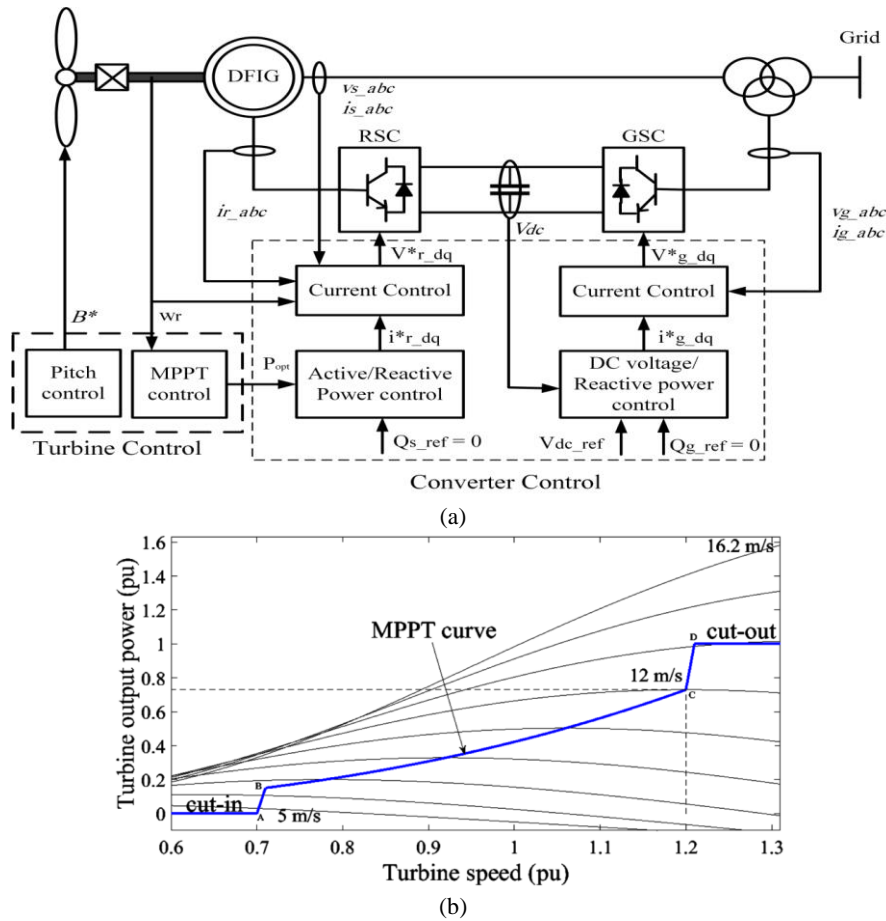


Figure 1. (a) DFIG wind turbine together with its controllers, (b) MPPT curve

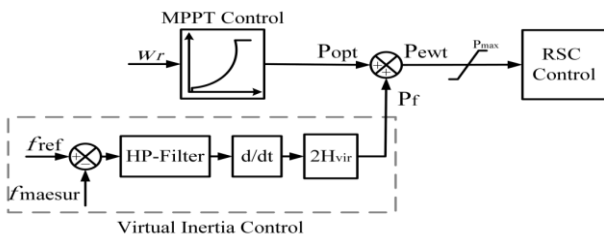


Figure 2. DFIG active power control integrated with VIC

As illustrated in Figure 1(a), in DFIGs, the rotor is jointed to the network through two back to back power electronic converters. They are usually modeled in form of PWM voltage source converters for injecting a controlled sinusoidal AC three phase voltage to the rotor windings. The converters should be able to work in both rectifier and inverter modes to provide bidirectional path for power flow between the rotor and network. The grid-side converter (GSC) is controlled to keep constant DC-link voltage and regulate the reactive power exchange between the converter and power grid. On the

other hand, the rotor-side converter (RSC) provides decoupled control of active and reactive powers of the generator [19]. The active power is conventionally controlled based on MPPT strategy where the wind turbine can work at variable rotor speeds for extracting the maximum wind power, according to Figure 1(b). In this strategy, if the wind speed exceeds a maximum allowable value, pitch angle controller limits the output power. Also, the reactive power can be independently controlled to support different grid requirements. However, due to limited capacity of the converters and providing unity power factor, the reference of reactive power is usually set to zero [18].

2. 2. Virtual Inertia Controller (VIC) The DFIG with traditional MPPT control provide no inertial response to the network frequency events. Figure 2 shows a typical VIC for DFIG wind turbine. It is a derivative controller that provides a transient inertial response for the DFIG active power through the stored kinetic energy of the rotor. The performance of the VIC is specified by the virtual inertia gain (H_{vir}). Moreover, a

first-order high-pass filter is usually used to activate the controller only when there are significant frequency deviations. In this way, the DFIG's rotor motion equation can be expressed as follows [9, 10]:

$$P_{m_{wt}} - P_{e_{wt}} = 2H_{wt} \frac{d\omega_r}{dt} = 2H_{wt} \frac{d\omega_r}{d\omega_s} \times \frac{d\omega_s}{dt} = 2H_{vir} \frac{d\omega_s}{dt} \quad (7)$$

where H_{vir} is as:

$$H_{vir} = H_{wt} \frac{d\omega_r}{d\omega_s} \cong H_{wt} \frac{\Delta\omega_r}{\Delta\omega_s} = H_{wt} \eta \quad (8)$$

According to Equation (8), the virtual inertia directly depends on $\eta = \Delta\omega_r/\Delta\omega_s$ where $\Delta\omega_r$ and $\Delta\omega_s$ are the angular speed variations of the wind turbine and power system, respectively. As explained before, the DFIG has a wide range of speed regulation from ω_{r_cut-in} to $\omega_{r_cut-off}$. On the other hand, the traditional synchronous generators usually work quite close to the synchronous speed ω_s to keep the system frequency stability. Therefore, considering that $\Delta\omega_r$ is much larger than $\Delta\omega_s$, and then $\eta \gg 1$, the increased penetration of DFIG wind farms provides a significant potential for network frequency regulation.

3. COORDINATED DESIGN OF VIC AND INTER-AREA OSCILLATION DAMPING

3. 1. Analysis of The Relationship Between System Inertia Response and Inter-Area Oscillations

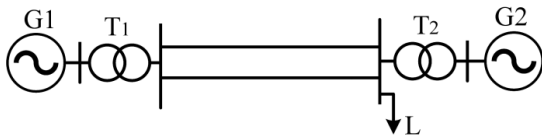


Figure 3. Single line diagram of two-area network

In this section, the dynamic equations of a typical regional power network are developed to analyse the relationship between the system inertia and inter-area oscillations. For example, a two-area power network is considered as depicted in Figure 3, where G_1 and G_2 are the equivalent generators in the feeding side and receiving side, respectively. The swing equations of each generator are given below [20]:

$$2H_i \frac{d\omega_i}{dt} = P_{m_i} - P_{e_i} - D_i (\omega_i - 1) \quad (9)$$

$$\frac{d\delta_i}{dt} = \omega_0 (\omega_i - 1)$$

where $i = 1, 2$ denotes the generator number.

In Equation (9), the electric output power of G_1 and G_2 can be calculated as follows [20]:

$$P_{e_1} = E_1'^2 G_{11} + E_1' E_2' (G_{12} \cos \delta_{12} + B_{12} \sin \delta_{12})$$

$$P_{e_2} = E_2'^2 G_{22} + E_1' E_2' (G_{12} \cos \delta_{12} - B_{12} \sin \delta_{12}) \quad (10)$$

where $\delta_{12} = \delta_1 - \delta_2$ is the load angle between two networks, G_{11} and G_{22} are the equivalent internal conductance of G_1 and G_2 , respectively. G_{12} and B_{12} are the transfer conductance and susceptance between G_1 and G_2 , respectively.

By considering the mechanical power is constant and replacing Equation (10) into Equation (9), the state equations of the system for a small perturbation around operating point are obtained as follows [21]:

$$2H_1 \frac{d\Delta\omega_1}{dt} = -K_1 \Delta\delta_{12} - D_1 \Delta\omega_1 \quad (11)$$

$$2H_2 \frac{d\Delta\omega_2}{dt} = -K_2 \Delta\delta_{12} - D_2 \Delta\omega_2 \quad (12)$$

$$\frac{d\Delta\delta_{12}}{dt} = \omega_0 (\Delta\omega_1 - \Delta\omega_2) \quad (13)$$

where

$$K_1 = E_1' E_2' (-G_{12} \sin \delta_{12} + B_{12} \cos \delta_{12})$$

$$K_2 = E_1' E_2' (-G_{12} \sin \delta_{12} - B_{12} \cos \delta_{12}) \quad (14)$$

Based on Equations (11)-(13), the system dynamics depend on the inertia parameters. To evaluate the impacts of these parameters on stability of inter-area oscillations, a reduced-order model based on the integral manifold theory can be used to integrate and eliminate unneeded differential equations. Accordingly, the system reduced-order model is derived as follows [22]:

$$\begin{bmatrix} p \Delta\delta_{12} \\ p \Delta\omega_{12} \end{bmatrix} = \begin{bmatrix} -a_1 \omega_0 & (1-a_2) \omega_0 \\ -K_1/2H_1 & -D_1/2H_1 \end{bmatrix} \begin{bmatrix} \Delta\delta_{12} \\ \Delta\omega_{12} \end{bmatrix} \quad (15)$$

where $\Delta\delta_{12}$ and $\Delta\omega_{12}$ are the states of the reduced-order model system, and respectively specify the rotor angle deviations and angular speed deviations between two areas. Also, p is the derivative operator. From Equation (15), the system characteristic equation is obtained as:

$$p^2 + \left(a_1 \omega_0 + \frac{D_1}{2H_1} \right) p + \frac{\omega_0}{2H_1} [a_1 D_1 + (1-a_2) K_1] = 0 \quad (16)$$

Subsequently, the system eigenvalues are given by:

$$p_{1,2} = \alpha \pm \beta i \quad (17)$$

where the real part of the system eigenvalues is calculated as follows:

$$\alpha = -\frac{1}{2} \left(a_1 \omega_0 + \frac{D_1}{2H_1} \right) \quad (18)$$

In general, the real parts of eigenvalues play major role in damping of system oscillations, such that if they become more negative, the damping will be increased. According to Equation (18), in a regional power network, the eigenvalues' real part (α) is inversely related to the inertia gain of the feeding side (H_1). Consequently, it can be concluded that supporting more virtual inertia from DFIG wind farm may increase the inter-area oscillations.

3. 2. Adaptive Inertia Control for Improving Power System Oscillations

Based on what has been explained so far, it can be stated that although supporting more inertia by DFIG can improve the frequency stability, however, the damping of inter-area oscillations will likely reduce. Hence, in this section, we intend to propose a novel adaptive VIC for DFIG wind turbines to simultaneously handle both the inter-area oscillations and frequency stability.

The inter-area oscillations in a regional network can be specified by the angular speed deviations between the areas. For example, for the two-area system shown in Figure 3, the inter-area oscillations is considered as $\Delta\omega_{12}=\Delta\omega_1-\Delta\omega_2$. This is a global signal that can be obtained using the wide-area measurements [23]. In the oscillatory conditions, one period of $\Delta\omega_{12}$ can be divided into four stages, as represented in Figure 4. In stages I and III, the amplitude of $\Delta\omega_{12}$ is increasing and a larger inertia can restrict it. In return, in stages II and IV, its amplitude is declining and a lower inertia will accelerate the oscillation damping. Thus, an adaptive VIC can help to damp the inter-area oscillations. In a practical manner, the stages I to IV can be recognized

through the signals of $\Delta\omega_{12}$ and its derivative, as given in Table 1.

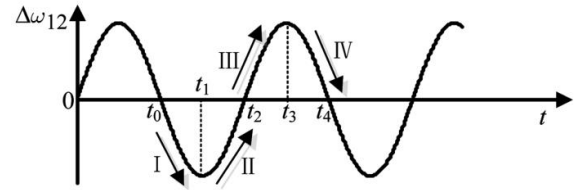


Figure 4. Oscillation stages of $\Delta\omega_{12}$

TABLE 1. Adaptive inertia control for inter-area oscillation damping

Stage	$\Delta\omega_{12}$	$d(\Delta\omega_{12})/dt$	H_{vir}
I	Negative	Negative	High
II	Negative	Positive	Low
III	Positive	Positive	High
IV	Positive	Negative	Low

3. 3. Designing the Adaptive VIC for DFIG Using Fuzzy Logic Method

To implement the controllers with the imprecise inputs and linguistic control patterns, the fuzzy logic is the most suitable approach. The fuzzy logic controllers do not require an accurate mathematical model of the system and the design criteria are linguistic rules. The fuzzy rules are universally determined based on human experience from the desirable control actions. They can also provide robust performance under nonlinear circumstances [24].

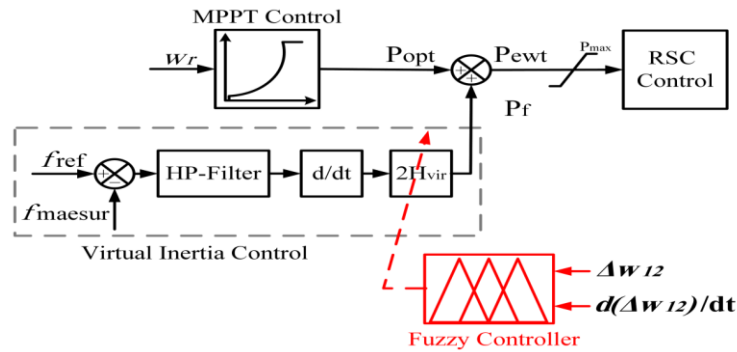


Figure 5. Schematic of the proposed fuzzy adaptive VIC

In this section, an adaptive VIC is designed for DFIG wind turbines using fuzzy logic method. The proposed fuzzy VIC can help to damp the inter-area oscillations in regional power networks according to the discussion presented in the previous section. Figure 5 represents the block diagram of the DFIG's active power controller integrated with the proposed fuzzy VIC. In this scheme, the virtual inertia gain (H_{vir}) is adaptively regulated with respect to the angular speed deviations between two

areas ($\Delta\omega_{12}$) and its change rate ($d\Delta\omega_{12}/dt$).

Every fuzzy controller consists of three parts called as fuzzification, fuzzy inference mechanism, and defuzzification [25]. Fuzzification is the procedure of converting the crisp input variables into the corresponding fuzzy values. The membership functions (MFs) determine the degree of belonging of the input variables to one of the fuzzy sets. Here, two MFs (i.e., Negative and Positive) are employed to fuzzify each of

the two input variables, according to Figures 6(a) and 6(b), respectively. In the next step, the fuzzy inference system deduces the fuzzy output based on the available fuzzy rules. The implication of fuzzy rules requires a sufficient knowledge and experience about the practical system. They are expressed by a set of linguistic statements linking a limited number of conditions with a limited number of consequences. In this study, the appropriate control actions are obtained using the fact that the high inertia is needed when the inter-area oscillations are increasing, and the low inertia adjustments require when the oscillations are approaching to the steady state values. Accordingly, two MFs are considered for the fuzzy output as "High" or "Low", which can be seen in Figure 6(c). The fuzzy inference system is used the Mamdani type and the Max-Min method to deduce the fuzzy output [25]. In addition, four fuzzy rules are applied as follows:

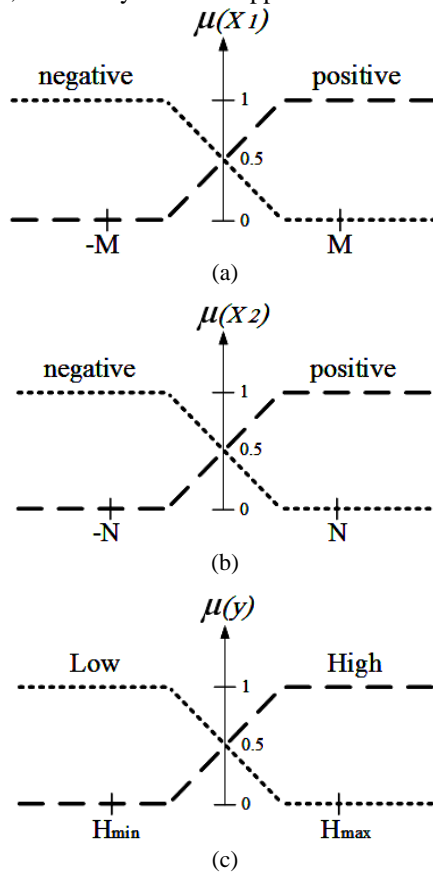


Figure 6. Input and output fuzzy MFs: (a) $X_1 = \Delta\omega_{12}$ (b) $X_2 = d(\Delta\omega_{12})/dt$ (c) $y = H_{vir}$

Rule (1): IF ($\Delta\omega_{12}$ is "Negative") AND ($d\Delta\omega_{12}/dt$ is "Negative") THEN (H_{vir} is "High")

Rule (2): IF ($\Delta\omega_{12}$ is "Negative") AND ($d\Delta\omega_{12}/dt$ is "Positive") THEN (H_{vir} is "Low")

Rule (3): IF ($\Delta\omega_{12}$ is "Positive") AND ($d\Delta\omega_{12}/dt$ is "Positive") THEN (H_{vir} is "High")

Rule (4): IF ($\Delta\omega_{12}$ is "Positive") AND ($d\Delta\omega_{12}/dt$ is "Negative") THEN (H_{vir} is "Low")

Finally, the centroid defuzzifier is used to convert the fuzzy output into the corresponding crisp output signal, as follows [25]:

$$H = \frac{\sum_{j=1}^4 \mu(y_j) \cdot y_j}{\sum_{j=1}^4 \mu(y_j)} \tag{20}$$

For optimal design of the fuzzy controller, the parameters of the inputs and output MFs (M, N, H_{min}, H_{max}) are determined through genetic algorithm (GA) [26, 27]. To do so, the integral time-weighted absolute error (ITAE) is considered as the performance index [28]. It defines by

$$ITAE = \int_0^{\infty} |\Delta\omega_{12}(t)| t dt \tag{21}$$

The ITAE integrates the absolute error multiplied by the time over time. The ITAE has the best selectivity considering that the oscillations settle much more quickly than the other tuning methods such as integral squared error (ISE) and integral absolute error (IAE) [28].

Figure 7 depicts the flowchart of GA optimization process [26]. The optimization is started by randomly generating an initial population. The initial population includes 20 chromosomes each consisting of 4 gens which are associated to the MFs parameters. Afterward, the selection, crossover and mutation operations take place to reproduce the next generation. Through selection, the chromosomes with high fitness are replicated in the next generation while those with low fitness will be fewer or not at all. Crossover is to take more than one parent solution and produce a child from them. In this operation, a chromosome is divided into two parts and recombined with another chromosome with the same crossover point. Mutation randomly changes a gene of a chromosome to maintain the genetic diversity from one generation to the next. Finally, the old generation is replaced with the new one. This procedure is repeated until the termination condition is fulfilled. At the end, the chromosome with minimum performance index will be selected as the best solution.

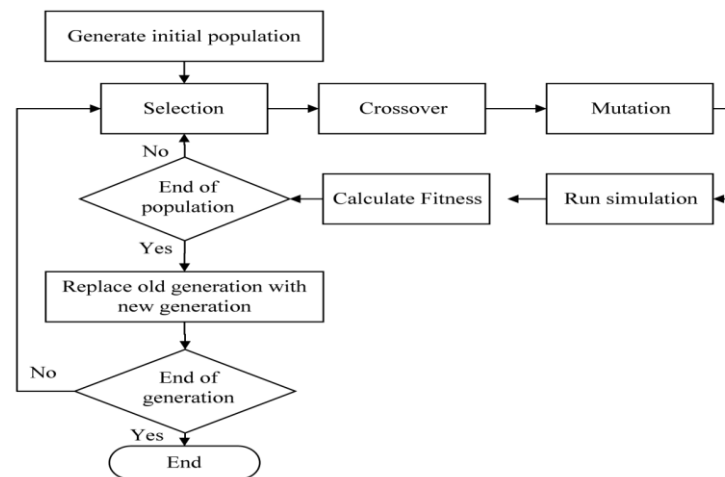


Figure 7. The GA Flowchart

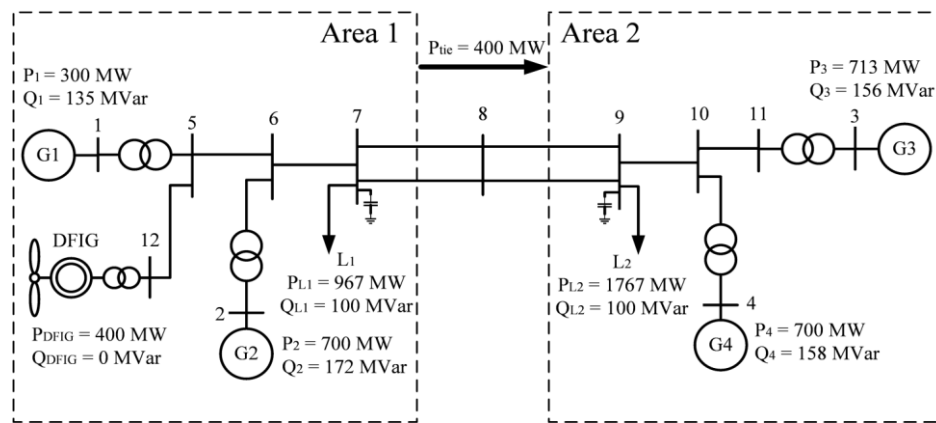


Figure 8. The test system

4. SIMULATION STUDIES

In this section, the dynamic performance of the proposed fuzzy adaptive VIC is evaluated using simulation studies. The test system is a generic two-area power network, as depicted by Figure 8 [20]. The area 1 contains two conventional synchronous generators (G_1 and G_2), one aggregated load (L_1) and one DFIG wind farm. The area 2 also includes two conventional synchronous generators (G_3 and G_4) and one aggregated load (L_2). The nominal capacity of the generation units and the loads are seen in Figure 8. Also, as marked in this figure, the area 1 nominally sends about 400 MW to the area 2 via the power tie-lines. The wind farm was modelled as a single equivalent wind turbine with capacity of 400MW (80 units of 5 MW) and unity power factor. It is worth noting that although the wind farm practically includes a large number of wind turbines, however, considering each individual wind turbine in the modelling process raises the complexity and simulation time. To overcome this problem, the aggregation method is used in this paper [18].

In the next subsections, the modal analysis results and the time domain transient responses are presented as the comparative studies between the following three cases:

- *Case 1*: DFIG without VIC
- *Case 2*: DFIG with fixed gain VIC
- *Case 3*: DFIG with fuzzy adaptive VIC

4. 1. Modal Analysis The test system was simulated in MATLAB/Simulink software and its linear state-space model was extracted by using the *linmod* command. Based on that, Table 2 lists the electromechanical oscillatory modes of the system. The modes of 1 and 2, respectively represent the local oscillatory modes of the areas 1 and 2, while the mode 3 is associated with the inter-area oscillations. This study intends to focus on the inter-area oscillatory mode of the system with frequency 0.439 Hz and damping ratio 3.15%. With this regards, Table 3 implies the normalized participation factor of each synchronous generator in the inter-area oscillatory mode [29]. As can

be seen, G_1 and G_3 have the highest participation factor in the inter-area oscillations. In addition, Table 4 compares the inter-area oscillatory modes of the test system when the DFIG operates with different inertia control strategy. It is observed that the DFIG equipped with the fixed gain VIC decreases the damping ratio from 3.15 to 2.54%, while the proposed adaptive VIC increases it to 10.42%. However, in all the three cases, there is no considerable change in the oscillation frequency.

4. 2. Time-Domain Simulations To compare the system transient behaviours with the three cases 1, 2 and 3, the results of time domain simulations are presented for different frequency events such as sudden loss of generation and short circuit fault with load shedding.

4. 2. 1. Transient Behaviours Under Loss of Generation At first, a sudden loss of generation by 250 MW of G_2 is considered to occur. Following this event, the system frequency experiences a temporary fall. The minimum frequency directly affects the system frequency stability during the transient process. According to Figure 9(a), the minimum frequency of the system increases when the DFIG wind farm operates in cases 2 and 3. Therefore, both cases 2 and 3 can offer better frequency stability compared to case 1.

TABLE 2. Electromechanical oscillatory modes

Mode No.	Eigenvalue	Frequency (Hz)	Damping ratio (%)	Oscillation mode
1	$-0.6217 \pm 6.5097i$	1.0360	9.51	Local (#1)
2	$-0.6539 \pm 7.2618i$	1.1557	8.97	Local (#2)
3	$-0.0870 \pm 2.7591i$	0.4391	3.15	Inter-area

TABLE 3. Normalized participation factor in inter-area oscillations

Generator	G_1	G_2	G_3	G_4
Participation factor	0.66	0	1	0.09

TABLE 4. Inter-area oscillatory modes for different virtual inertia control strategy

	Eigenvalue	Frequency (Hz)	Damping ratio (%)
Case 1	$-0.0870 \pm 2.7591i$	0.4391	3.15
Case 2	$-0.0693 \pm 2.7168i$	0.4324	2.54
Case 3	$-0.2742 \pm 2.6175i$	0.4166	10.42

This is due to the inertial response of DFIG active power, as shown in Figure 9(b). It is observed that in cases 2 and 3, the DFIG active power changes dynamically to support the system frequency, while it stays almost constant in case 1.

Figures 9(c) and 9(d) respectively represent the oscillations between two sub-regional networks in terms of the angular speed deviation between G_1 and G_3 ($\Delta\omega_{12}$) and the active power passing through the tie-lines between the buses 7 and 9 (P_{79}). It is worth noting that G_1 and G_3 are the generators with the highest participation in the inter-area oscillation mode, as previously indicated in Table 3. The figures reveal that both the amplitude and time of oscillations are increased in case 2, while they are effectively suppressed in case 3. This achieves by the adaptive control performance of the proposed VIC with respect to the inter-area oscillations, as shown in Figure 9(e). This is while that in case 2, the DFIG supports the fixed virtual inertial response during the frequency event.

To provide a quantitative comparison between the three cases, the graphs of Figures 10(a)-10(c) respectively compares the minimum network frequency (f_{min}), the maximum absolute deviation of $\Delta\omega_{12}$ ($\max|\Delta\omega_{12}|$) and its settling time (Δt_s). Figure 10(a) indicates that the minimum frequency in case1 is 59.65 Hz, while it increases to 59.77 and 59.76Hz in cases 2 and 3, respectively. On the other hand, Figures 10(b) and 10(c) demonstrate that the adaptive fuzzy VIC (case 3) decreases the $\max|\Delta\omega_{12}|$ and Δt_s by 29 and 54% relative to case1, respectively. However, the fixed gain VIC (case 2) increases them from 0.425 to 0.428 (rad/s) and 6.38 to 7.22 (s), respectively.

4. 2. 2. Transient Behaviours under Short Circuit Fault with Load Shedding

In the second test, a three-phase to ground short-circuit fault is considered to occur in the middle of one of the tie-lines at $t=2$ s and to be cleared after 100 ms by opening the circuit breakers at two ends of the faulty line. Then, 200 MW load shedding of L_2 will be immediately imposed to avoid overloading the healthy line. Under this circumstance, breaking the tie-line between two networks results in the inter-area oscillations, and the load shedding increases the system frequency.

Figures 11(a)-11(d) represent the transient behaviours of the system in terms of the system frequency (f), the DFIG active power (P_{DFIG}), the angular speed deviation between G_1 and G_3 ($\Delta\omega_{12}$), and the active power of tie-lines between buses 7 and 9 (P_{79}), respectively. As shown in Figure 11(a), both the fixed and adaptive VICs are successful to restrict the maximum frequency and its change rate.

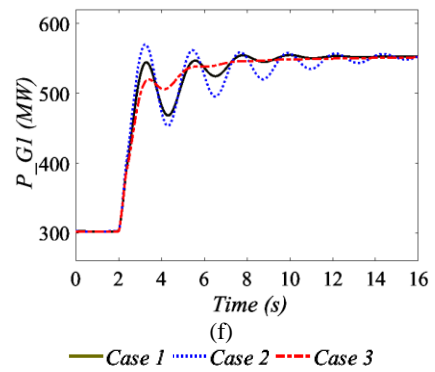
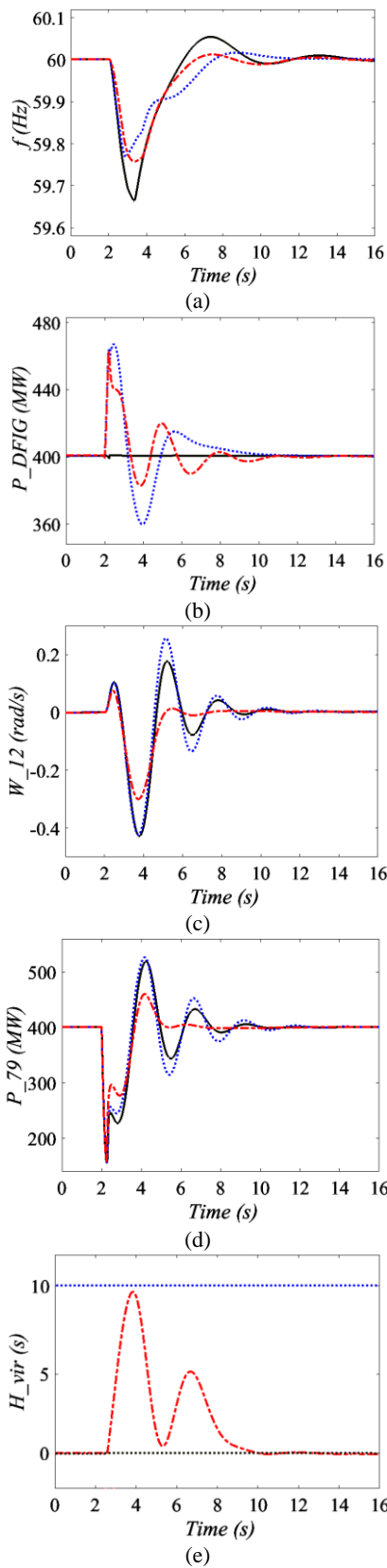


Figure 9. Transient behaviors under sudden loss of generation: (a) network frequency (b) DFIG active power (c) angular speed deviation between G_1 and G_3 (d) inter-area power oscillation (e) virtual inertia gain (f) active power of G_1

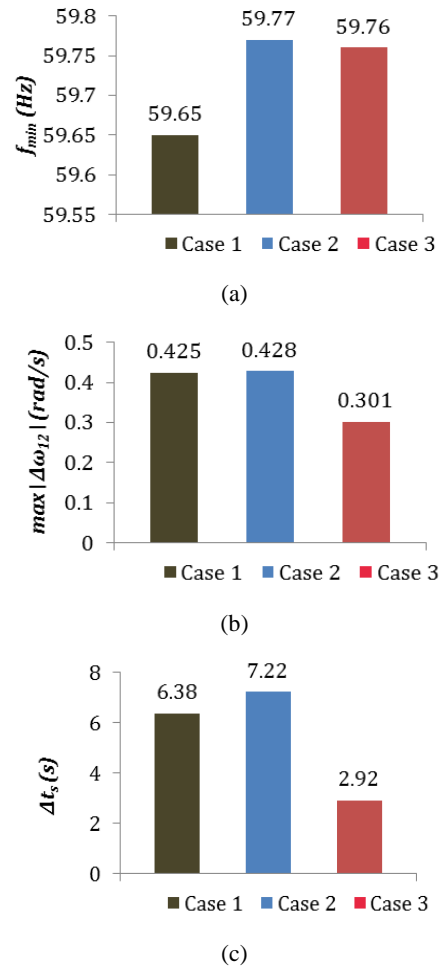


Figure 10. The quantitative comparison under loss of generation: (a) minimum frequency, (b) maximum absolute deviation of $\Delta\omega_{12}$, (c) settling time of $\Delta\omega_{12}$

On the other hand, Figures 11(c) and 11(d) reveals that the use of the proposed adaptive VIC can dramatically reduce the system inter-area oscillations, while the fixed gain VIC increases them for both of the amplitude and time of oscillations. Figures 12(a)-12(c) provide the quantified comparative results between the three case as the bar graphs. According to Figure 11(a), the maximum frequency decreases from 60.69 Hz in case 1 to 60.43 and 60.38 Hz in cases 2 and 3, respectively. Also, Figure 12(b) indicates that the maximum absolute deviation of $\Delta\omega_{12}$ in case 3 is decreased about 22% relative to case 1. In addition, it can be seen in Figure 12(c) that in case 3 the settling time of inter-area oscillations decreases by 43% relative to case 1, while it increases by 10% in case 2.

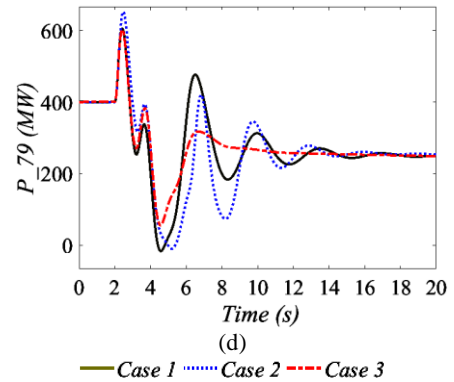
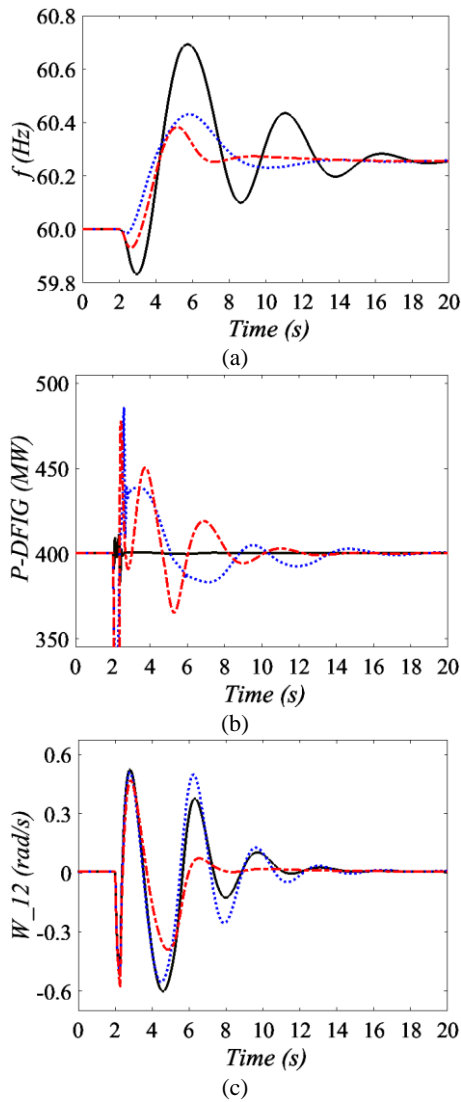


Figure 11. Transient behaviors under short circuit disturbance with load shedding: (a) network frequency (b) DFIG active power (c) angular speed deviation between G_1 and G_3 (e) inter-area power

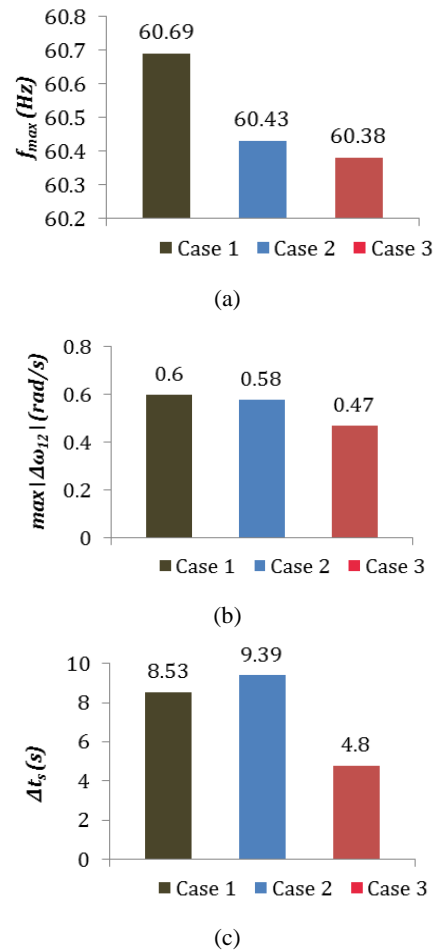


Figure 12. The quantitative comparison under short circuit with load shedding: (a) maximum frequency, (b) maximum absolute deviation of $\Delta\omega_{12}$, (c) settling time of $\Delta\omega_{12}$

5. CONCLUSION

This paper revealed the increased penetration of DFIG wind farm equipped with the traditional fixed gain VIC may increase the inter-area oscillations of regional power networks. To solve this problem, a novel adaptive VIC was proposed in this paper. In the proposed VIC, the virtual inertia gain is not fixed and dynamically adjusted using fuzzy logic with respect to inter-area oscillations. The effectiveness and control performance of the proposed adaptive fuzzy VIC was verified through different simulation studies under loss of generation, short circuit fault and load shedding. All the results confirm the DFIG equipped with the proposed fuzzy VIC can provide better performance than the traditional fixed gain VIC for both the inter-area oscillations damping and frequency stability.

6. REFERENCES

- Cheng, M., and Ying, Z., "The state of the art of wind energy conversion systems and technologies: A review", *Energy Conversion and Management*, Vol. 88, (2014), 332-347.
- Douadi, T., Y. Harbouche, R. Abdessemed, and I. Bakhti, "Improvement performances of active and reactive power control applied to DFIG for variable speed wind turbine using sliding mode control and FOC." *International Journal of Engineering- Transactions A: Basics*, Vol. 31, No.10, (2018), 1689-1697.
- Kayikçi, M., and Jovica V. M., "Dynamic contribution of DFIG-based wind plants to system frequency disturbances" *IEEE Transactions on Power Systems*, Vol. 24, No. 2, (2009), 859-867.
- Gautam, D., Goel, L., Ayyanar, R., Vittal, V. and Harbour, T., "Control strategy to mitigate the impact of reduced inertia due to doubly fed induction generators on large power systems" *IEEE Transactions on Power Systems*, Vol. 26, No. 1, (2011), 214-224.
- Muyeen, S. M., Rion Takahashi, Toshiaki Murata, and Junji Tamura, "A variable speed wind turbine control strategy to meet wind farm grid code requirements" *IEEE Transactions on Power Systems*, Vol. 25, No. 1 (2010), 331-340.
- Ochoa, D., and Sergio, M., "Fast-Frequency Response provided by DFIG-Wind Turbines and its impact on the grid" *IEEE Transactions on Power Systems*, Vol. 32, (2017), 4002-4011.
- Dreidy, M., Mokhlis, H., and Mekhilef, S., "Inertia response and frequency control techniques for renewable energy sources: A review" *Renewable and Sustainable Energy Reviews*, Vol. 69, (2017), 144-155.
- Morren, J., De Haan, S.W., Kling, W.L. and Ferreira, J.A., "Wind turbines emulating inertia and supporting primary frequency control" *IEEE Transactions on Power Systems*, Vol. 21, No. 1 (2006), 433-434.
- Wu, Yuan-Kang, Wu-Han Yang, Yi-Liang Hu, and Phan Quoc Dung, "Frequency regulation at a wind farm using time-varying inertia and droop controls." *IEEE Transactions on Industry Applications*, Vol. 55, No. 1, (2019), 213-224.
- Attya, A. B., Dominguez-Garcia, J. L. and Anaya-Lara, O., "A review on frequency support provision by wind power plants: Current and future challenges." *Renewable and Sustainable Energy Reviews*, Vol. 81, (2018), 2071-2087.
- Zhang, Z.S., Y-Z. Sun, Jin Lin, and G-J. Li, "Coordinated frequency regulation by doubly fed induction generator-based wind power plants" *IET Renewable Power Generation*, Vol. 6, No. 1, (2012), 38-47.
- Sun, Y.Z., Zhang, Z.S., Li, G.J. and Lin, J., "Review on frequency control of power systems with wind power penetration", *International Conference on Power System Technology, IEEE*, (2010), 1-8.
- Pulgar-Painemal, H., and Galvez-Cubillos, R., "Wind farms participation in frequency regulation and its impact on power system damping" *Power Technology (POWERTECH), 2013 IEEE Grenoble*, (2013).
- Zhang, X., Y. Fu, S. Wang, and Y. Wang, "Effects of two-area variable inertia on transient stabilisation in interconnected power system with DFIG-based wind turbines" *IET Renewable Power Generation*, Vol. 11, No. 5, (2017), 696-706.
- Gayme, D. F., and Chakraborty, A., "Impact of wind farm placement on inter-area oscillations in large power systems" *American Control Conf (ACC), 2012 IEEE*, 2012.
- Miao, Z., Fan, L., Osborn, D. and Yuvarajan, S., "Wind farms with HVdc delivery in inertial response and primary frequency control" *IEEE Transactions on Energy Conversion*, Vol. 25, No. 4, (2010), 1171-1178.
- Xi, X., Hua, G., and Geng, Y., "Small signal stability of weak power system integrated with inertia tuned large scale wind farm" *Innovative Smart Grid Technologies-Asia (ISGT Asia), 2014 IEEE*, 2014.
- Fernández, L. M., Jurado, F., and Saenz, J. R., "Aggregated dynamic model for wind farms with doubly fed induction generator wind turbines" *Renewable Energy*, Vol. 33, No. 1, (2008), 129-140.
- Wu, F., Zhang, X.P., Godfrey, K. and Ju, P., "Small signal stability analysis and optimal control of a wind turbine with doubly fed induction generator" *IET Generation, Transmission & Distribution*, Vol. 1, No. 5 (2007), 751-760.
- Kundur P., Power system stability and control. *New York: McGraw Hill*, (1994).
- Xiangyi, Ch., Li Ch., and Wang, Y., "Analysis of the inter-area low frequency oscillations in large scale power systems" *6th IEEE Conference on Industrial Electronics and Applications*, (2011), 1627-1631.
- Sauer, P. W., Ahmed-Zaid, S., and Kokotovic, P. V. "An integral manifold approach to reduced order dynamic modeling of synchronous machines" *IEEE Transactions on Power Systems*, Vol. 3, No. 1 (1988), 17-23.
- Asgharia, R., Mozafari, S. B., Amraeeb, T., "Delay-Scheduled Controllers for Inter-Area Oscillations Considering Time Delays" *International Journal of Engineering-Transactions B: Applications*, Vol.31, No.11, (2018), 1852-1861.
- Zadeh, L.A., Fuzzy sets. *Information and control*, Vol. 8, No. 3, (1965), 338-353.
- Momoh, J. A., Ma, X. W., and Tomsovic, K., "Overview and literature survey of fuzzy set theory in power systems" *IEEE Transactions on Power Systems*, Vol. 10, No. 3, (1995), 1676-1690.
- Man, K. F., Tang, K. S., and Kwong, S., "Genetic algorithms: concepts and applications [in engineering design]" *IEEE Transactions on Industrial Electronics*, Vol. 43, No. 5, (1996), 519-534.
- Lashkar Ara, A., Bagheri Tolabi, H., and Hosseini, R., "Dynamic modeling and controller design of distribution static compensator in a microgrid based on combination of fuzzy set

and galaxy-based search algorithm." *International Journal of Engineering-Transactions A: Basics*, Vol. 29, No.10, (2016), 1392-1400.

28. Schultz, W. C., and Rideout, V. C., "Control system performance measures: Past, present, and future." *IRE Transactions on Automatic Control*, Vol. 1, (1961), 22-35.

29. Pal, B., Chaudhuri, B. Robust control in power systems, *Springer*, (2006)

Coordinated Control of Doubly Fed Induction Generator Virtual Inertia and Power System Oscillation Damping Using Fuzzy Logic

A. R. Solat^a, A. M. Ranjbar^b, B. Mozafari^a

^a Department of Electrical and Computer Engineering, Science and Research Branch, Islamic Azad University, Tehran, Iran

^b Department of Electrical Engineering, Sharif University of Technology, Tehran, Iran

PAPER INFO

Paper history:

Received 31 December 2018

Received in revised form 02 February 2019

Accepted 07 March 2019

Keywords:

Doubly Fed Induction Generator Wind

Turbine

Virtual Inertia Control

Frequency Stability

Inter-area Oscillation

Fuzzy Logic

چکیده

توربین‌های بادی مبتنی بر DFIG با کنترل سنتی MPPT نمی‌توانند پاسخ اینرسیایی موثری به اختلالات فرکانسی شبکه داشته باشند. اخیراً با افزایش ظرفیت تولیدات بادی، استراتژی کنترل اینرسی مصنوعی DFIG به منظور پشتیبانی از پایداری فرکانسی شبکه متصل شده، پیشنهاد شده است. با این حال، در این مقاله نشان داده می‌شود که کنترل اینرسی مصنوعی متداول با بهره‌ثابت، اثرات منفی بر میرایی نوسانات بین ناحیه‌ای در شبکه‌های قدرت چند ناحیه‌ای دارد. برای مقابله با این مشکل، در این مقاله، یک کنترل‌کننده اینرسی مصنوعی تطبیقی مدرن به منظور کنترل هماهنگ پاسخ اینرسی DFIG و میرایی نوسانات بین ناحیه‌ای شبکه قدرت پیشنهاد می‌شود. در طرح پیشنهادی، بهره VIC ثابت نیست بلکه با استفاده از منطق فازی و به طور تطبیقی با توجه به نوسانات بین ناحیه‌ای شبکه تنظیم می‌شود. عملکرد و کارایی کنترل‌کننده اینرسی مصنوعی فازی پیشنهادی در شرایط اختلالات فرکانسی مختلف نظیر فقدان ناگهانی تولید، خطای اتصال کوتاه و قطع بار، ارزیابی می‌شود. همچنین مطالعات شبیه‌سازی روی یک سیستم قدرت دو ناحیه‌ای استاندارد که یک مزرعه بادی به آن متصل شده است انجام می‌شود و نتایج به صورت مقایسه‌ای برای سه مورد ارائه می‌شوند: 1) DFIG بدون کنترل اینرسی مصنوعی، 2) DFIG با کنترل اینرسی مصنوعی با بهره ثابت، 3) DFIG با کنترل اینرسی مصنوعی تطبیقی فازی. تمام نتایج بدست آمده تأیید می‌کنند که کنترل‌کننده اینرسی مصنوعی پیشنهادی، علاوه بر بهبود پایداری فرکانسی سیستم قدرت به طور همزمان میرایی نوسانات بین ناحیه‌ای را نیز افزایش می‌دهد.

doi: 10.5829/ije.2019.32.04a.11